Atmospheric
Measurement
Techniques

An integrated approach toward the incorporation of clouds in the temperature retrievals from microwave measurements

F. Navas-Guzmán, O. Stähli, and N. Kämpfer

Institute of Applied Physics (IAP), University of Bern, Bern, Switzerland

Correspondence to: F. Navas-Guzmán (francisco.navas@iap.unibe.ch)

Abstract. In this paper, we address the characterization of clouds and its inclusion in microwave retrievals in order to study its effect on tropospheric temperature profiles measured by TEMPERA radiometer. TEMPERA is the first ground-based microwave radiometer that makes it possible to obtain temperature profiles in the troposphere and stratosphere at the same time. In order to characterize the clouds a multi-instrumental approach has been adopted. Cloud base altitudes were detected using ceilometer measurements while the integrated liquid water was measured by TROWARA radiometer. Both instruments are co-located with TEMPERA in Bern (Switzerland). Using this information and a constant Liquid Water Content value inside the cloud a liquid profile is provided to characterize the clouds in the inversion algorithm. Microwave temperature profiles have been obtained incorporating this water liquid profile in the inversion algorithm and also without considering the clouds, in order to assess its effect on the retrievals. The results have been compared with the temperature profiles from radiosondes which are launched twice a day at the aerological station of MeteoSwiss in Payerne (40 km W of Bern). Almost 1 year of data have been analysed and 60 non-precipitating cloud cases were studied. The statistical analysis carried out over all the cases evidenced that temperature retrievals improved in most of the cases when clouds were incorporated in the inversion algorithm.

1 Introduction

The importance of the knowledge of the temperature structure in the atmosphere has been widely recognized. Temperature is a key parameter for dynamical, chemical and radiative processes in the atmosphere. In the troposphere the atmospheric temperature profiles are important for weather fore- and now-casting. Different techniques allow the measurement of atmospheric temperature profiles via radiosonde, Fourier transform infrared spectroscopy (FTIR), lidar or satellite and ground-based microwave radiometers. The main advantage of microwave radiometers over other instruments is the high temporal resolution with a reasonably good spatial resolution. Moreover, measurement at a fixed location makes it possible to observe local atmospheric dynamics over a long time period.

Ground-based microwave radiometers for tropospheric temperature profiles are well established and exist in different configurations (Stähli et al., 2013). Some examples are MICCY (microwave radiometer for cloud cartography) (Crewell et al., 2001), RPG-HATPRO (Radiometer Physics GmbH-Humidity and Temperature Profiler) (Rose et al., 2005), Radiometrics MP-3000A (Ware et al., 2003) and ASMUWARA (All-Sky MUltiWAvelength RAdiometer) (Martin et al., 2006).

Many studies have addressed the characterization of the temperature in the troposphere using microwave radiometer measurements (Basili et al., 2001; Stähli et al., 2013; Löhnert and Maier, 2012). However, despite the presence of clouds in many atmospheric observations, only a few studies have dealt with the incorporation of clouds in the temperature retrievals (Löhnert et al., 2004; Solheim et al., 1998; Ware et al., 2003). A better knowledge of cloud characterization as well as of the assessment of its effect on temperature under different cloudy conditions is still needed. The work presented here addresses the characterization of clouds and its incorporation into the temperature retrievals for almost 1 year of measurements.

The paper is organized as follows. In Sect. 2, the instrumentation and the measurements are described. The methodology used to characterize the clouds and its inclusion in the retrievals are presented in Sect. 3. Section 4 presents the results obtained for almost one year of measurements. Finally the conclusions are found in Sect. 5.

2　Instrumentation and measurements

Temperature profiles are provided using the radiometer called TEMPERA. This instrument is a heterodyne receiver at a frequency range of 51–57 GHz. Figure 1 shows a picture of TEMPERA which is operated in a temperature-stabilized laboratory at the ExWi Building of the University of Bern (Bern, Switzerland; 575 m above sea level; 46.95° N, 7.44° E, azimuth view direction: southeast (131.5°)). In this lab a styrofoam window allows views of the atmosphere over the zenith angle (za) range from 30 to 70°. The instrument mainly consists of three parts: a front end to collect and detect the microwave radiation, with two back ends: a filter bank and a digital FFT spectrometer for the spectral analysis. Technical details about the antenna, the signal treatment in the front end and calibration can be found in Stähli et al. (2013).

For tropospheric measurements we use a filter bank with four channels. By adjusting a local oscillator (LO) frequency with a synthesizer it is possible to measure at 12 frequencies which are listed in Table 1. In this way we cover uniformly the range 51–57 GHz at positions between the emission lines (see Fig. 2). The lower nine channels have a band-width of 250 MHz and the channels 10–12 have a bandwidth of 1 GHz to enhance the sensitivity in the flat spectral region.

The second back end is used for stratospheric measurements and contains a digital FFT spectrometer (Acqiris AC 240) for the two emission lines centred at 52.5424 and 53.0669 GHz. Stratospheric retrievals are not addressed in this paper. A detailed description of this back end and the stratospheric retrievals can be found in Stähli et al. (2013).

The measurements are performed in periodic cycles of 60 s. Each cycle starts with a hot load calibration in combination with a noise diode for 9 s followed by the atmosphere measurements. They consist of two parts: first a 15 s period at a zenith angle za = 30° to observe with the FFT spectrometer and simultaneously with the filter bank, and second, a tipping curve in 3 s periods and angular steps in 5° up to za = 70°. After calibration, the output of each measurement cycle is a set of 108 brightness temperatures of the filter bank at 12 frequencies and at nine zenith angles. For the tropospheric retrieval we use a mean of 15 measurement cycles leading to a time resolution of 15 min (Stähli et al., 2013).

The cloud characterization has been performed using different instrumentation. Integrated liquid water (ILW) was measured by means of the radiometer TROWARA that is installed next to TEMPERA. Since 2002, TROWARA has
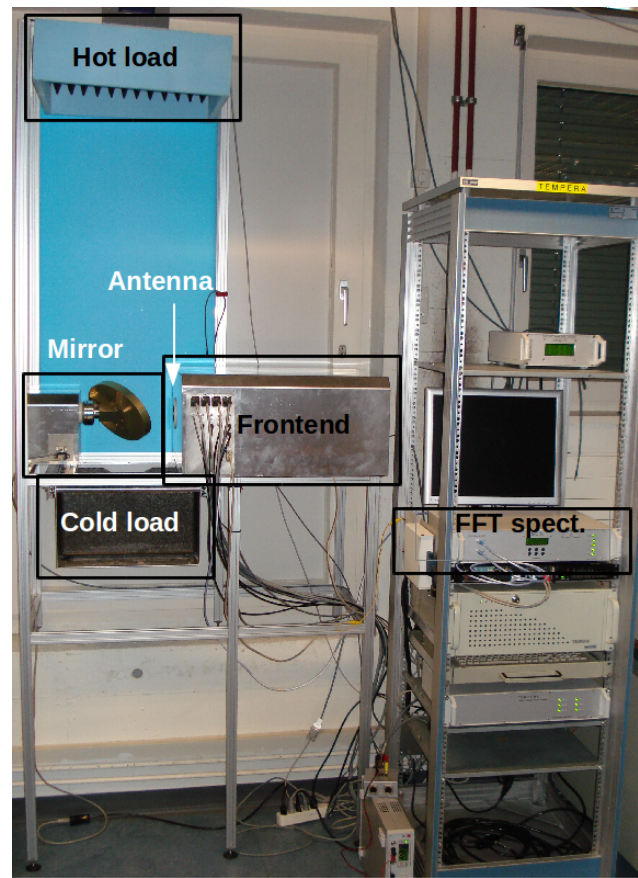

Figure 1. TEMPERA at the laboratory at ExWi, Bern (Switzerland).

operated in a temperature-controlled room, looking into the atmosphere (elevation angle of 40°) through a styrofoam window. This radiometer measures the radiation from the sky in the same direction at 21, 22 and 31 GHz. A detailed description about this instrument and the inversion algorithms is presented by Matzler and Morland (2009).

A Vaisala CT25K ceilometer was used to measure the cloud base heights. This instrument employs a pulsed diode laser that emits at 905 nm. The backscatter radiation caused by haze, fog, mist, precipitation and clouds is measured as the laser pulses traverse the sky. The resulting backscatter profile, i.e. signal strength versus height, is stored and processed and the cloud bases are detected. The elevation angle of the ceilometer has been set to 40 deg to guarantee the observation of clouds inside of TEMPERA field of view.

Independent in situ temperature measurements performed by means of radiosondes have been used in this study. These radiosondes are regularly launched twice a day at 11:00 and 23:00 UTC in the atmospheric survey station in Payerne (46.82° N, 6.95° E; 491 m above sea level and 40 km southwest of Bern). The station belongs to MeteoSwiss.
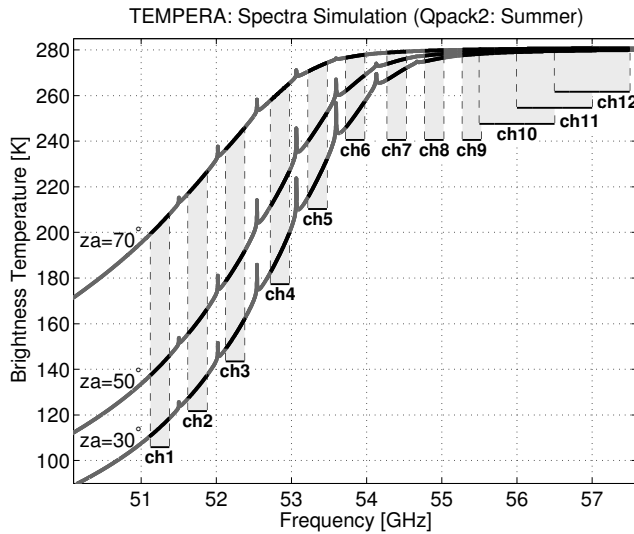
Figure 2. TEMPERA spectrum of 51–57 GHz simulated with Qpack2/ARTS2 during summer for zenith angles at 30, 50 and 70°. The grey bars indicate the 12 channels (ch1–ch12) of the filter bank.

3 Methodology

3.1 Retrieval

The TEMPERA radiometer measures thermal radiation of 51–57 GHz on the wing of the 60 GHz oxygen-emission region of the microwave spectrum. Oxygen is a well-mixed gas whose fractional concentration is independent of altitude below approx. 80 km. Therefore, the radiation contains information primarily on atmospheric temperature.

A ground-based microwave radiometer measures a superposition of emission and absorption of radiation at different altitudes. The received intensity at ground level can be expressed in the Rayleigh–Jeans limit ($h\upsilon << kT$) in terms of the brightness temperature T_B. In these conditions the radiative transfer equation is given by

$$T_B(h_0, \upsilon, \theta) = T_0 e^{-\tau(\upsilon, h_1)}$$
$$+ \int_{h_0}^{h_1} T(h) e^{-\tau(\upsilon, h)} \alpha(\upsilon, h) \frac{1}{\cos(\theta)} dh, \quad (1)$$

where $T_B(\theta)$ is the brightness temperature at zenith angle θ, T_0 is the brightness temperature of the cosmic background radiation, $T(h)$ is the physical temperature at height h, h_0 is the Earth surface, h_1 is the upper boundary in the atmosphere, α is the absorption coefficient and τ is the opacity. The opacity is defined as

$$\tau(\upsilon, h) = \int_{h_0}^{h} \alpha(\upsilon, h') dh'. \quad (2)$$

Table 1. Frequencies (f) and bandwidths (B) of tropospheric channels (ch1–ch12).

Channel	f [GHz]	B [MHz]	Channel	f [GHz]	B [MHz]
1	51.25	250	7	54.40	250
2	51.75	250	8	54.90	250
3	52.25	250	9	55.40	250
4	52.85	250	10	56.00	1000
5	53.35	250	11	56.50	1000
6	53.85	250	12	57.00	1000

From Eq. (1) we see that it is possible to calculate the estimated brightness temperature from the state of the atmosphere (forward modelling). A more difficult task is to solve the inverse problem: given the measured brightness temperatures, what is the physical temperature profile that gave rise to them?

In this study the measured spectrum is inverted to a temperature profile by the optimal estimation method (OEM) (Rodgers, 2000) using the radiative transfer model ARTS/QPack (Eriksson et al., 2011). This principle is based on Bayes' probability theorem. A detailed description of this method as applied to our system can be found in Stähli et al. (2013).

To solve the inverse problem we use the Gauss–Newton iterative method, whose solution can be expressed in a matrix notation as follows:

$$x_{i+1} = x_i + \left(S_a^{-1} + K_i^T S_\epsilon^{-1} K_i^{-1} \right)$$
$$\left[K_i^T S_\epsilon^{-1} (y - F(x_i)) - S_a^{-1} (x_i - x_a) \right], \quad (3)$$

where the vector x is the true temperature profile, y is the measured spectrum (brightness temperature), x_a is the a priori temperature profile, S_a is the a priori covariance matrix and S_ϵ is the observation error covariance matrix. The use of the forward model in this equation is noted by F and the vector K is the weighting function ($K = \partial F / \partial x$).

In the radiative transfer calculations we use the model of Rosenkranz and the model of Liebe for the absorption coefficient calculations: Rosenkranz (1998) for H_2O, Rosenkranz (1993) for O_2 and Liebe et al. (1993) for N_2 (Stähli et al., 2013). A tropospheric water vapour profile with an exponential decrease is included. This profile is calculated with the measured surface water vapour density from the ExWi weather station (placed next to TEMPERA) and assuming a scale height of 2000 m (Bleisch et al., 2011). For other species like oxygen (O_2) and nitrogen (N_2) we used standard atmospheric profiles for summer and winter (Anderson et al., 1986), which are incorporated into ARTS2.

Figure 3 shows the absorption coefficient for oxygen, water vapour, liquid water and nitrogen for five different frequencies between 51 and 57 GHz. The absorption coefficient for oxygen, water vapour and nitrogen was calculated for the atmospheric conditions found at 23:00 UTC on
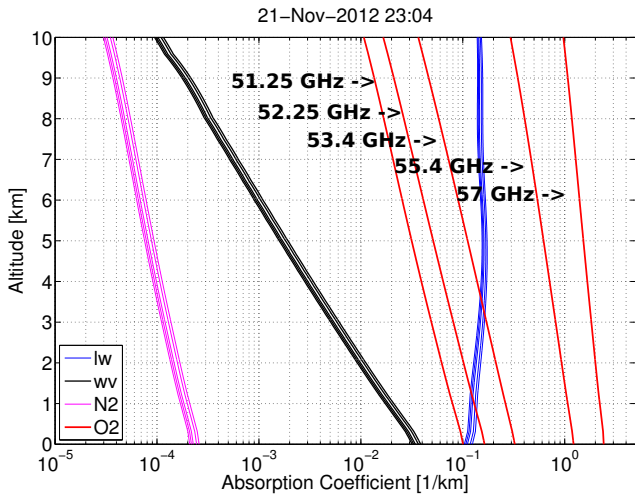
Figure 3. Vertical profiles of absorption coefficients for oxygen (O_2), water vapour (wv), liquid water (lw) and nitrogen (N_2) at 51.25, 52.25, 53.4, 55.4 and 57 GHz calculated for atmospheric conditions on 21 November 2012 in Bern.

21 November 2012 in Bern. From this plot we observe that the spectral dependency in this range is very small for water vapour, liquid water and nitrogen. This is not true for oxygen, which is strongly dependent on frequency. Moreover, we observe that under cloudless conditions (ILW = 0), most of the absorption and emission in the atmosphere comes from oxygen dominating the contribution from water vapour and nitrogen. For the liquid water the absorption coefficient was calculated assuming a constant liquid water profile up to 10 km in order to assess its relevance at different altitudes. From this plot we observe that the clouds have a strong influence in the frequency range from 51 to 54 GHz and their absorptions and emissions cannot be considered negligible. Moreover, the liquid water absorption coefficient increases slightly with the altitude indicating that clouds get more important at higher altitudes.

Despite its importance, the influence of liquid water in the forward model has not been sufficiently treated due to the difficulty of characterizing the clouds. Stähli et al. (2013) proposed to reduce its effect on the forward model using only the measured frequencies larger than 53 GHz, which are less affected by clouds. This improved the temperature retrievals, as shown by a comparison with radiosondes. However, the discrepancies between temperature profiles from microwave radiometers and from radiosondes were still considerable.

3.2 Cloud characterization

A multi-instrumental approach has been used in order to characterize the clouds. All the instruments used for this purpose are co-located at the ExWi Building of the University of Bern. Cloud base altitudes (CBAs) were detected using a Vaisala CT25K ceilometer that is continuously operated.

The instrument points to the atmosphere with an elevation angle of 40°. The base of the cloud is detected using a derivative method, which identifies a maximum gradient in the backscattered signal at the base cloud altitude.

The ILW was measured by TROWARA radiometer under the same observational elevation angle as the ceilometer (40°). The presence of clouds was assumed for those cases with ILW larger than 0.025 mm.

An important parameter to characterize the clouds is the liquid water content (LWC). This parameter indicates the mass of liquid water per unit volume of air and is usually expressed in $g\,m^{-3}$. Different authors have characterized the LWC for different kinds of clouds (Hess et al., 1998; Korolev et al., 2007; Rosenfeld and Lensky, 1998). Cirrus and fog present much lower water content than other kinds of clouds, with values around 0.03 and $0.06\,g\,m^{-3}$, respectively. In a continental environment, the LWC values are around $0.26\,g\,m^{-3}$ for cumulus, $0.28\,g\,m^{-3}$ for stratus and between 1.0 and $3.0\,g\,m^{-3}$ for cumulonimbus, depending on whether they are growing or dissipating (Hess et al., 1998; Rosenfeld and Lensky, 1998). In this study we have assumed a constant LWC value of $0.28\,g\,m^{-3}$ inside the clouds. This value is characteristic of stratus, which are the most typical clouds found in this study. An analysis of the sensitivity of the temperature retrievals for different LWC values will be presented in the next section.

Knowing the ILW and the LWC values it is possible to get directly the cloud thickness (Δz) from

$$\text{ILW} = \text{LWC} \times \Delta z. \qquad (4)$$

Moreover, using the information of the cloud base altitude retrieved from the ceilometer and the cloud thickness it is possible to provide a LWC profile (Fig. 4) to the forward model in order to study its effect on the temperature retrievals.

4 Results

As indicated in the previous sections, continuous radiometer and ceilometer measurements are performed at the ExWi Building of the University of Bern. Moreover, radiosondes launched twice a day at 11:00 and 23:00 UTC at Payerne (40 km W of Bern) were available. In this study temperature profiles retrieved from TEMPERA radiometer have been compared with in situ temperature measurements performed by radiosondes. Due to the limitations in the radiosonde launches just two profiles are compared per day.

Almost 1 year of data, from February to December of 2012, has been analysed in this study. A total of 60 no-precipitating cloud cases were found. In order to study the cloud effect on the temperature retrievals, the profiles have been calculated including and not including a LWC profile in the forward model.
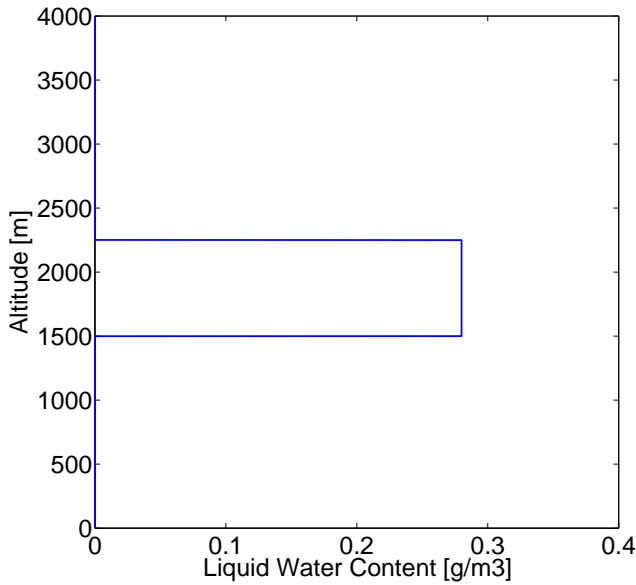
Figure 4. Example of LWC profile incorporated in the forward model corresponding to an ILW of 0.21 mm.

4.1 Case studies

From the 60 cases, three clear situations have been identified regarding the location and thickness of the clouds. The first one corresponds to the presence of thick clouds at medium and high altitudes. The second one is when the clouds are thin and are located at medium and high altitudes and the third one is when there is presence of low clouds.

Figure 5a shows the temperature profiles retrieved from radiosonde and from TEMPERA radiometer using and without using cloud information in the forward model. The measurements were done on 21 November 2012 and an ILW value of 0.47 mm was measured with TROWARA for these cloudy conditions. Figure 5b presents the absolute temperature deviation between the radiosondes and the radiometer retrievals. For this case the cloud base altitude was detected at 2450 m (a.s.l.) and the cloud thickness was 1670 m. From the figure we observe a very good agreement between radiosonde and radiometer retrievals when the cloud was considered. The mean absolute temperature deviation in the first kilometre reached an average value of 0.8 ± 0.6 K. Although the discrepancies increased a little bit above this altitude, the mean absolute deviation was always below 3 K in the whole profile. However, we can observe that the discrepancies between the radiosonde and the microwave profile retrieved without cloud information are much larger. Although the agreement was reasonable in the lower profile, the discrepancies increased considerably above 1300 m (a.s.l.), reaching a maximum absolute deviation of 9.2 K at 4480 m (a.s.l.). Figure 5c shows the corresponding brightness temperatures for the different retrievals. A total of 108 measured brightness temperatures are shown corresponding to
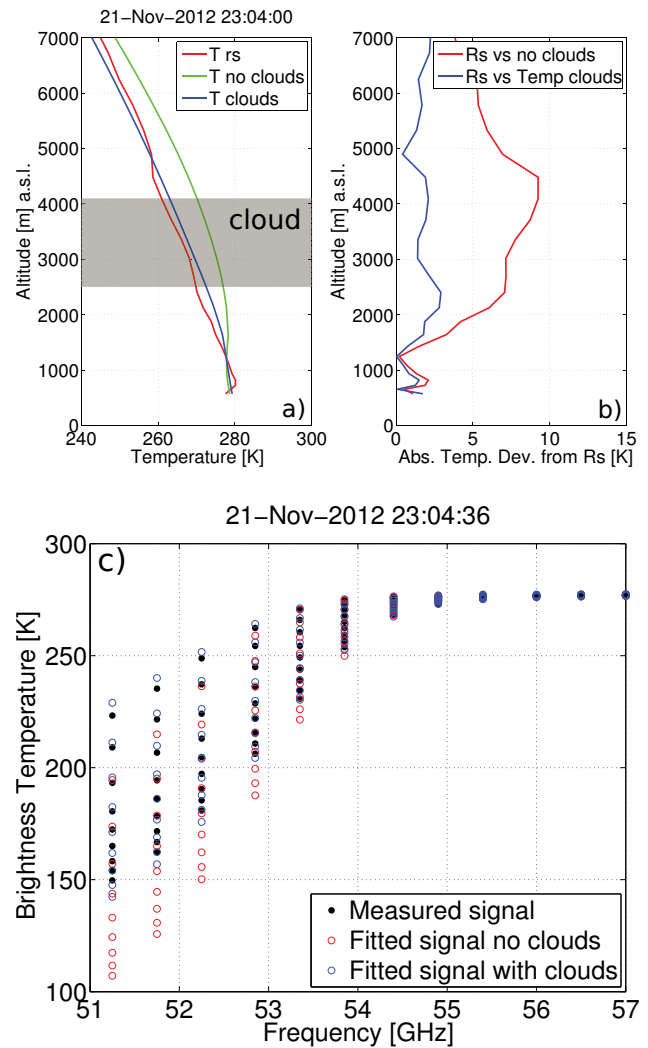

Figure 5. (a) Temperature profiles on 21 November 2012 retrieved from radiosonde (red line) and from TEMPERA radiometer using and not using cloud information in the forward model (blue and green lines, respectively). The cloud is marked with a grey box. **(b)** Absolute temperature deviation for inversions with clouds (blue line) and without clouds (red line) from radiosondes. **(c)** Measured brightness temperatures and forward model brightness temperatures obtained using and not using clouds in the retrievals.

the measurements from the 12 channels under nine observational zenith angles (black points). In addition, the forward model brightness temperatures for the retrievals with and without clouds, blue and red circles respectively, are also presented. We can observe that the forward model brightness temperatures for the retrieval including the cloud information agree much better with the measured brightness temperature than do those obtained without cloud information. The absolute differences between measured and forward model brightness temperatures (residuals) are between 0.003 and 7 K for the retrieval with cloud and between 0.017 and 42.6 K for the retrieval without cloud. The plot also confirms that

the biggest discrepancies in the brightness temperatures between both retrievals are found for the lower frequencies (< 54 GHz), as could be predicted from the absorption coefficients (Fig. 3). It is also interesting to note that the changes in the brightness temperatures for the different zenith angles are small for the highest frequencies due to the large opacity from the oxygen at these frequencies. In conclusion, this example evidenced a clear improvement in both physical and brightness temperatures when cloud information was provided to the forward model.

Another atmospheric situation found in this study corresponded to the presence of thin clouds at medium and high altitudes. Figure 6 shows an example measured on 14 October 2012 at 23:01 UTC. The ILW value measured in this case was lower than in the previous one (0.03 mm). For this night a cloud with a thickness of 108 m was detected at the altitude of 4304 m (a.s.l.). From this figure a good agreement between the temperature profiles retrieved from radiometer measurements and from the radiosonde is observed (Fig. 6a). We can observe that under these conditions there is not a clear difference in the retrievals when the LWC profile is incorporated in the forward model. The mean absolute temperature deviations in the whole profile were 1.3 ± 0.7 K and 1.0 ± 0.6 K with clouds and without cloud information in the retrievals, respectively. These results evidence that thin clouds at medium and high altitudes do not modify significantly the brightness temperature measured at ground base (Fig. 6c).

Figure 7 shows an example of low clouds. The measurements were performed on 26 October 2012 at 11:06 UTC. A ILW value of 0.13 mm was measured with TROWARA. At this time a cloud of 481 m of thickness was detected at the altitude of 110 m (a.g.l.). In this situation the profiles retrieved from radiometer measurements showed different behaviour. While in the near range (below 1700 m, a.s.l.) both showed relatively good agreement with the radiosonde profile (maximum absolute deviation was lower than 1.9 K), above this altitude the profile retrieved using cloud information (blue line) showed bigger discrepancies with the radiosonde than the other one. The mean absolute temperature deviation between the radiosonde and the microwave profiles above 1.7 km were 3.1 ± 0.4 K with cloud and 0.8 ± 0.5 K without cloud information.

However, when the brightness temperatures were checked (Fig. 7c) we observed that the forward model brightness temperatures obtained for the retrieval with cloud agree better with the measured brightness temperatures than for the ones without cloud. This indicates that the microwave radiometer temperature retrieval also improved for this case when the cloud was incorporated, although the comparison of the physical temperature with the radiosonde does not prove that. This example evidences the difficulty of characterizing low clouds. The variability in the altitudes of low clouds is larger and in this sense the differences with the radiosonde can be important, as has been seen in this case. Moreover, to provide
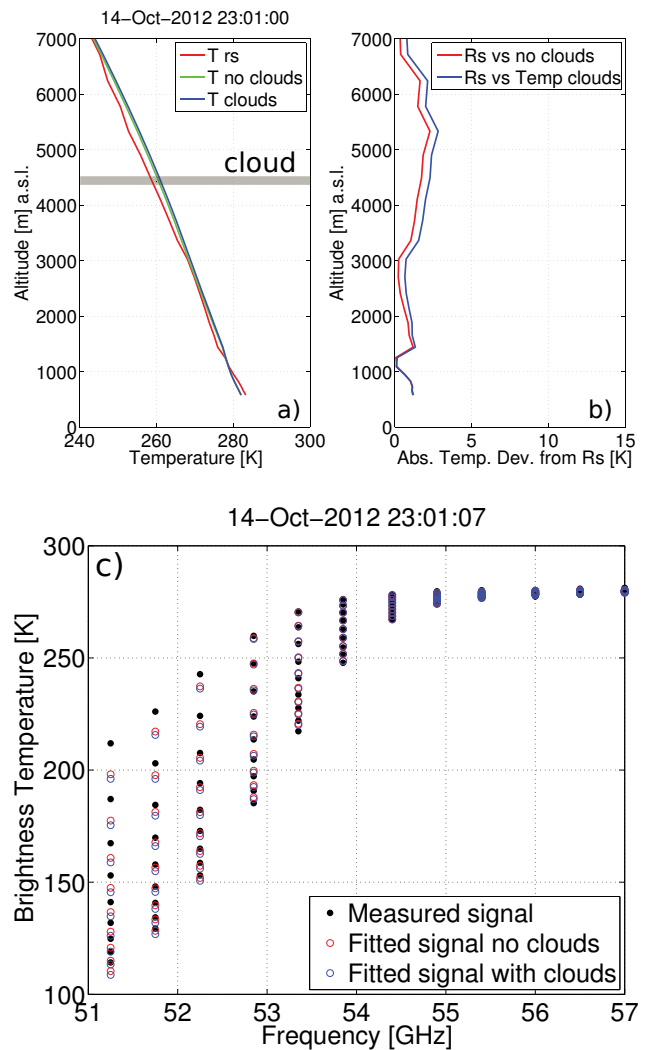

Figure 6. As in Fig. 5, but on 14 October 2012.

a wrong LWC profile (due to a mislocation of the cloud, possible stratification . . .) in the forward model could be more critical because the retrievals are more sensitive in the near range.

In order to assess the sensitivity of the temperature retrievals with the LWC value the three cases presented in this section have been checked considering very different kinds of clouds. The chosen LWC values for this test were 0.06, 0.28 and 1.0 g m^{-3} which are typical for cirrus, stratus and cumulonimbus, respectively. Table 2 presents the ILW value for each case and the different cloud thickness which are found depending on the kind of cloud. We can observe that for the same atmospheric conditions (with a fixed ILW value) the cloud thickness can range from some hundred metres to several kilometres depending on the kind of cloud.

Figure 8 shows different linear regressions obtained from temperature comparisons from radiosondes and microwave radiometer measurements for the three studied cases. The
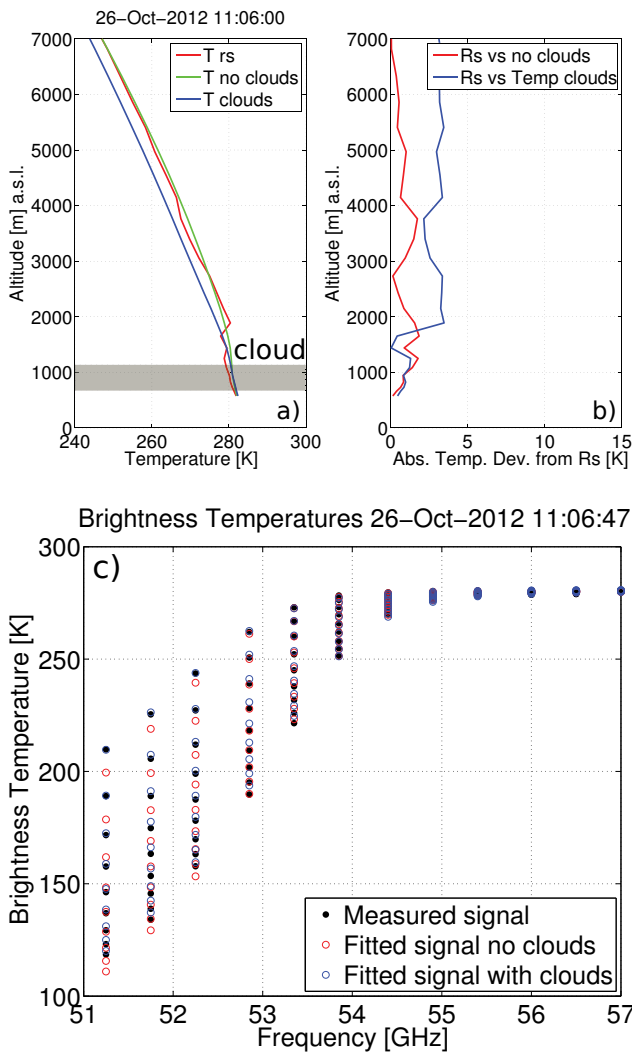
Figure 7. As in Fig. 5, but on 26 October 2012.

Table 2. ILW and cloud thickness for different kinds of cloud.

Date	ILW [mm]	Cirrus [m]	Stratus [m]	Cumulon. [m]
21 Nov	0.47	7770	1665	466
14 Oct	0.03	505	108	30
26 Oct	0.13	2246	481	134

4.2 Statistical study of temperature profiles

In this section a statistical analysis using the 60 cases of no precipitating clouds is performed. Figure 9 presents the mean absolute temperature deviation between radiosondes and microwave measurements using and without using the cloud information in the retrievals (blue and red lines, respectively). This figure shows that on average the differences in the temperature profiles from radiosondes and microwave radiometer are smaller when the clouds are incorporated in the forward model. It is also interesting to point out that the standard deviation is lower for the retrievals with clouds, indicating that this method reduces the variability in the differences. Moreover, we observe that the agreement of both radiometer retrievals is better in the lower than in the upper part of the troposphere. The mean absolute deviation is 0.88 ± 0.14 K below 2 km (a.s.l.), while it reaches 2.0 ± 0.4 K above this altitude for the retrievals with cloud information. The good agreement in the lower part evidences that the thermal structures in Payerne and Bern are very similar and it is reasonable to compare both instruments although they are located in different places. The bigger discrepancies in the upper part could be due to the lower resolution of the microwave radiometer in the far range. Similar discrepancies in the temperature were found in other studies where co-located radiosondes and microwave radiometers were compared. Güldner and Spänkuch (2001) reported differences of 0.7 K in the planetary boundary layer and 1.6 K at 7 km while Löhnert and Maier (2012) found discrepancies of 0.5 K in the lower boundary layer that increased to 1.7 K at 4 km height.

In order to better understand the cloud effect on the temperature retrievals we have classified the different cloud cases according to the amount of liquid water. Figure 10a shows the mean absolute deviation between radiometer and radiosondes for those cases with ILW lower than 0.04 mm. This condition was found in 13 cases. On average we can observe that there are no significant differences between both retrievals: the mean absolute deviation from the radiosonde in the range from ground to 7 km (a.s.l.) was 1.5 ± 0.3 K when the clouds were incorporated and 1.4 ± 0.3 K when they were not. These results show that the retrievals are not very sensitive for those clouds with a low LWC. Figure 10b corresponds to cases with ILW between 0.04 and 0.1 mm. A total of 19 cases were found in this range. We can observe that for this ILW range both microwave retrievals were almost identical below 2 km (a.s.l.) with a mean absolute deviation of
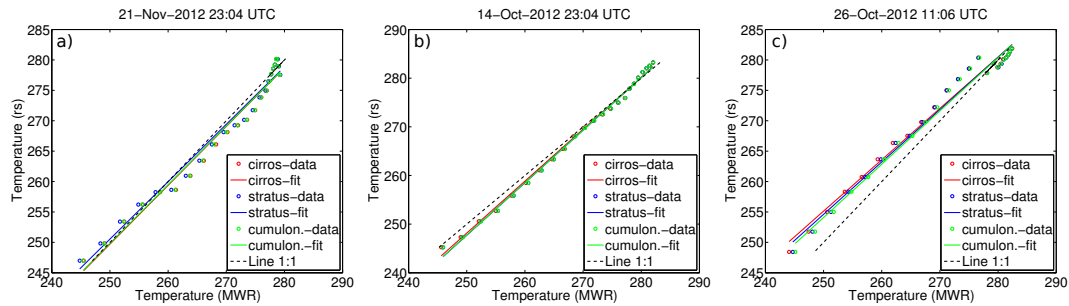
regressions presented correspond to temperatures measured in the height range between ground and 7 km. The microwave retrievals were performed using the LWC values indicated before for different kind of clouds. We can observe that despite the extreme LWC values used for the different kind of clouds the changes in the temperatures were very small. The correlation coefficients were larger than 0.99 in all regressions. The biggest discrepancies found in all the cases were always below 1 K, indicating that the temperature retrievals were not very sensitive to the LWC parameter. For this reason the statistical analysis presented in the next section was performed using the LWC value of 0.28 g m^{-3} which is typical for stratus. This kind of cloud was the most common found in our study.

Figure 8. Linear regressions between the temperatures from radiosondes and from microwave radiometer measurements on 21 November **(a)**, 14 October **(b)** and 26 October **(c)**. The microwave temperature retrievals incorporating clouds were calculated for typical LWC values for cirrus, stratus and cumulonimbus.
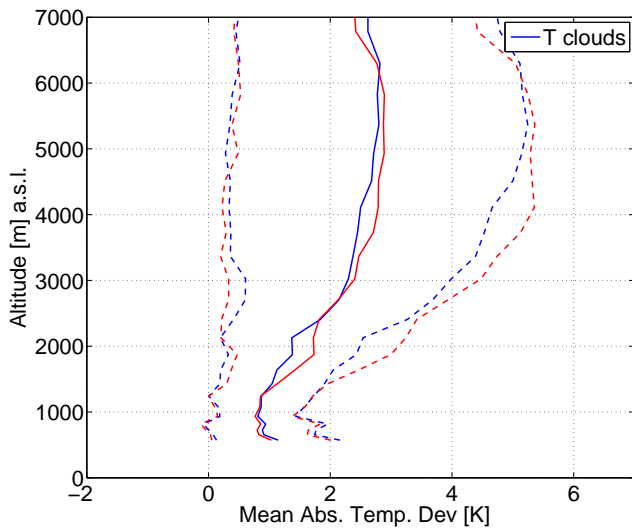

Figure 9. Mean absolute temperature deviation between radiosondes and microwave profiles. The blue line corresponds to retrievals with clouds and the red line without clouds. The standard deviations are marked by dashed lines.

Figure 10. Mean absolute temperature deviation between radiosondes and microwave profiles for different ranges of ILW.

0.9 ± 0.2 K from the radiosonde. Above this altitude we observe that the cloud retrievals show larger discrepancies regarding the radiosondes. The mean absolute deviation in this range was 2.1 ± 0.4 K with clouds and 1.5 ± 0.2 K without cloud information in the forward model. Figure 10c shows the results for ILW larger than 0.1 mm. From this plot we observe that the cloud retrievals show a better agreement with the radiosondes in almost the whole profile. The mean absolute deviations for the whole profile were 2.1 ± 1.1 K for the retrievals with clouds and 2.5 ± 1.4 K without clouds. It is important to note the representativity of these last results, since they correspond to almost 50 % of the cases (28 cases) and they evidence that there is an improvement in the retrievals when cloud information is incorporated into the forward model.

Finally, the studied cases were also classified according to their cloud base altitudes. Figure 11a shows the mean
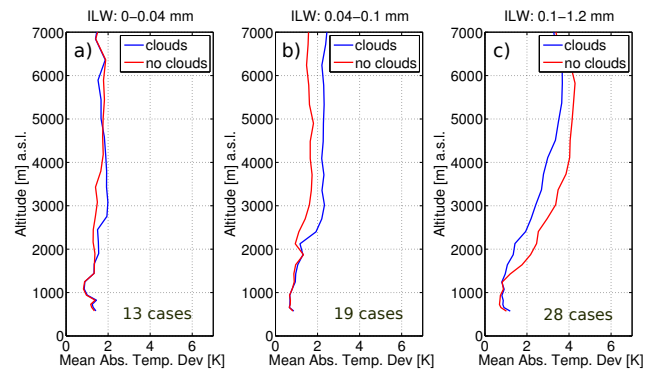
absolute deviation for the 22 cases with cloud base altitudes below 1000 m (a.g.l.). Different behaviour is observed in the near range than in the far range. Below 4 km (a.s.l.) the no-cloud retrievals show better agreement with radiosondes than when the clouds are included in the forward model. However, the behaviour is opposite above this altitude. For those cases with CBA between 1 and 3 km (a.g.l.) which correspond to almost 50 % of the cases (29) (Fig. 11b), the cloud retrievals show an improvement almost in the whole profile. For cases with CBA above 3 km (a.g.l.) (Fig. 11c) the retrievals show an opposite behaviour than for low clouds; the cloud retrievals present a better agreement below 4.2 km (a.s.l.) while it is worse above this altitude.

5 Conclusions

This work presents a study about the cloud effect on temperature profiles retrieved from microwave radiometry. So far, few studies have treated the clouds in the forward models and large differences are found for some cloudy conditions. Cloud characterization was carried out using different instrumentation. Cloud base altitude was retrieved using ceilometer measurements and the ILW was measured
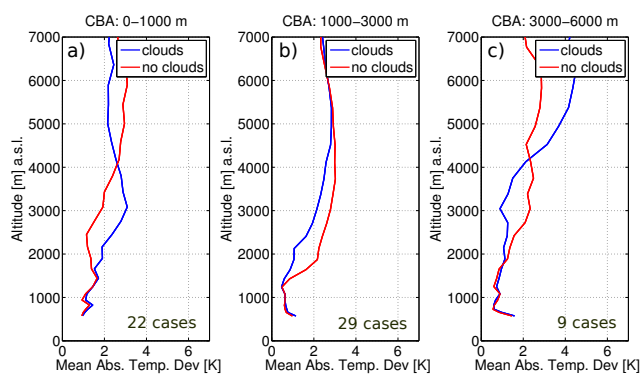
Figure 11. Mean absolute temperature deviation between radiosondes and microwave profiles for different ranges of cloud base altitudes.

using TROWARA radiometer. A constant LWC value of $0.28\,\mathrm{g\,m^{-3}}$ is used inside of the cloud. A LWC profile is provided to the forward model in order to take into account the clouds in the radiative transfer equation. Microwave temperature profiles have been obtained considering and without considering this LWC profile and they have been compared with radiosonde profiles. Almost 1 year of data has been analysed and a total of 60 non-precipitation cloud cases were found. Three different situations have been identified in the comparison of the microwave profiles with radiosondes. The first one corresponds to the presence of thick clouds at medium and high altitudes. For this situation a very good agreement between radiosonde and the retrievals with clouds was observed, while the discrepancies were much larger when the clouds were not considered. The second atmospheric situation found in this study corresponded to the presence of thin clouds at medium and high altitudes. In these conditions both microwave retrievals were very similar, showing that this kind of cloud does not significantly modify the measured brightness temperature at ground base. The third situation was the presence of low clouds. In this case the retrievals considering clouds did not show better results. They were even worse than the retrievals without clouds above 2 km (a.s.l.). However, the analysis of the forward model brightness temperatures for the retrievals with clouds evidenced a better agreement with the measured brightness temperatures. This indicated that the temperature retrievals improved when the clouds were incorporated and the differences with the radiosonde come from a real difference in the physical temperature for both locations. This illustrates the difficulty found in the analysis of low clouds since they present higher variability at low altitudes and the discrepancies with the radiosonde can be larger. The three cases were tested for different types of clouds (different LWC value) without showing significant differences in the retrievals.

A statistical analysis of all the cases showed that on average the microwave retrievals considering the clouds showed a better agreement with radiosondes with mean absolute deviations of 0.88 ± 0.14 K below 2 km (a.s.l.) and 2.0 ± 0.4 K above this altitude.

Moreover, different behaviours in the results were observed depending on the LWC of the clouds. For those cases with ILW lower than 0.1 mm there was not a clear improvement in the tropospheric retrievals when clouds were incorporated. However, for cases with ILW larger than 0.1 mm the retrievals with clouds showed a better agreement with the radiosondes in almost the whole profile. The mean absolute deviations from the radiosondes for the whole profile were 2.1 ± 1.1 K for the retrievals with clouds and 2.5 ± 1.4 K without clouds. These results evidenced the improvement in the temperature retrievals when clouds with high integrated liquid water are incorporated into the forward model.

The study also showed a different behaviour in the retrievals depending on the cloud base altitude. For cloud base altitudes below 1000 m (a.g.l.) and above 3000 m (a.g.l.) there was not a clear improvement when using cloud information in the retrievals. The difficulty of characterizing the low clouds due to their larger variability in the near range and the shift of the radiosonde in high altitudes could be the reason for these unclear results. Future campaigns where microwave radiometers operate at the same location as radiosondes are launched will help to improve the temperature retrievals for these atmospheric conditions. On the other hand we observed that the results were better for those cases with cloud base between 1000 and 3000 m (a.g.l.). This situation corresponded to almost 50 % of the cases.

References

Anderson, G. P., Clough, S., Kneizys, F., Chetwynd, J., and Shettle, E. P.: AFGL atmospheric constituent profiles (0.120 km), Tech. rep., DTIC Document, 1986.

Basili, P., Bonafoni, S., Ciotti, P., Marzano, F. S., d'Auria, G., and Pierdicca, N.: Retrieving atmospheric temperature profiles by microwave radiometry using a priori information on atmospheric spatial-temporal evolution, IEEE T. Geosci Remote, 39, 1896–1905, 2001.

Bleisch, R., Kämpfer, N., and Haefele, A.: Retrieval of tropospheric water vapour by using spectra of a 22 GHz radiometer, Atmos. Meas. Tech., 4, 1891–1903, doi:10.5194/amt-4-1891-2011, 2011.

Eriksson, P., Buehler, S., Davis, C., Emde, C., and Lemke, O.: ARTS, the atmospheric radiative transfer simulator, version 2, J. Quant. Spectrosc. Ra., 112, 1551–1558, 2011.

Güldner, J. and Spänkuch, D.: Remote sensing of the thermodynamic state of the atmospheric boundary layer by ground-based microwave radiometry, J. Atmos. Ocean. Tech., 18, 925–933, 2001.

Hess, M., Koepke, P., and Schult, I.: Optical properties of aerosols and clouds: The software package OPAC, B. Am. Meteorol. Soc., 79, 831–844, 1998.

Korolev, A., Isaac, G., Strapp, J., Cober, S., and Barker, H.: In situ measurements of liquid water content profiles in midlatitude stratiform clouds, Qu. J. Roy. Meteorol. Soc., 133, 1693–1699, 2007.

Liebe, H., Hufford, G., and Cotton, M.: Propagation modeling of moist air and suspended water/ice particles at frequencies below 1000 GHz, in: In AGARD, Atmospheric Propagation Effects Through Natural and Man-Made Obscurants for Visible to MM-Wave Radiation, 11 pp. (SEE N94-30495 08-32), Vol. 1, 1993.

Löhnert, U. and Maier, O.: Operational profiling of temperature using ground-based microwave radiometry at Payerne: prospects and challenges, Atmos. Meas. Tech., 5, 1121–1134, doi:10.5194/amt-5-1121-2012, 2012.

Löhnert, U., Crewell, S., and Simmer, C.: An integrated approach toward retrieving physically consistent profiles of temperature, humidity, and cloud liquid water, J. Appl. Meteorol., 43, 1295–1307, 2004.

Martin, L., Schneebeli, M., and Matzler, C.: ASMUWARA, a ground-based radiometer system for tropospheric monitoring, Meteorol. Z., 15, 11–17, 2006.

Matzler, C. and Morland, J.: Refined physical retrieval of integrated water vapor and cloud liquid for microwave radiometer data, IEEE T. Geosci Remote, 47, 1585–1594, 2009.

Rodgers, C. D.: Inverse methods for atmospheric sounding: Theory and Practice, Series on Atmospheric, Oceanic and Planetary Physics, Vol. 2, Singapole, World Scentic, 2000.

Rose, T., Crewell, S., Löhnert, U., and Simmer, C.: A network suitable microwave radiometer for operational monitoring of the cloudy atmosphere, Atmos. Res., 75, 183–200, 2005.

Rosenfeld, D. and Lensky, I. M.: Satellite-based insights into precipitation formation processes in continental and maritime convective clouds, B. Am. Meteorol. Soc., 79, 2457–2476, 1998.

Rosenkranz, P. W.: Absorption of microwaves by atmospheric gases, in: Atmospheric remote sensing by microwave radiometry, edited by: Janssen, M. A., John Wiley & Sons, New York, 37–90, ISBN 0471628913, 1993.

Rosenkranz, P. W.: Water vapor microwave continuum absorption: A comparison of measurements and models, Radio Sci., 33, 919–928, 1998.

Solheim, F., Godwin, J. R., Westwater, E., Han, Y., Keihm, S. J., Marsh, K., and Ware, R.: Radiometric profiling of temperature, water vapor and cloud liquid water using various inversion methods, Radio Sci., 33, 393–404, 1998.

Stähli, O., Murk, A., Kämpfer, N., Mätzler, C., and Eriksson, P.: Microwave radiometer to retrieve temperature profiles from the surface to the stratopause, Atmos. Meas. Tech., 6, 2477–2494, doi:10.5194/amt-6-2477-2013, 2013.

Ware, R., Carpenter, R., Güldner, J., Liljegren, J., Nehrkorn, T., Solheim, F., and Vandenberghe, F.: A multichannel radiometric profiler of temperature, humidity, and cloud liquid, Radio Sci., 38, 8079, doi:10.1029/2002RS002856, 2003.